Snow Water Equivalent Retrieval in a Canadian Boreal Environment From Microwave Measurements Using the HUT Snow Emission Model

Vincent Roy, *Member, IEEE*, Kalifa Goïta, Alain Royer, Anne E. Walker, and Barry E. Goodison

***Abstract*—Snow water equivalent (SWE) is a critical parameter for climatological and hydrological studies over northern high-latitude areas. In this paper, we study the usability of the Helsinki University of Technology (HUT) snow emission model for the estimation of SWE in a Canadian boreal forest environment. The experimental data (airborne passive microwave and ground-based data) were acquired during the Boreal Ecosystem-Atmosphere Study winter field campaign held in February 1994 in Central Canada. Using the experimental dataset, surface brightness temperatures at 18 and 37 GHz (vertical polarization) were simulated with the HUT snow emission model and compared to those acquired by the airborne sensors. The results showed an important underestimation at 37 GHz (-27 K) and an overestimation at 18 GHz (10 K). In this paper, we demonstrate that the errors in the model simulations are due mainly to the extinction coefficient modeling, which is a function of snow grain size. Therefore, we propose a new semiempirical function for the extinction coefficient, based on an empirical correction to the Rayleigh scattering expression. Results presented in this paper show that the proposed function improves the HUT model accuracy to predict brightness temperature in the experimental context considered, with a mean error of ± 5 K and ± 9 K, respectively, at 18 and 37 GHz, and a negligible bias (less than 4 K) in both cases. These errors are comparable in magnitude to the accuracy of the radiometers used during the airborne flights. SWE was retrieved using the modified HUT snow emission model based on an iterative inversion technique. SWE was estimated with a mean error of ± 10 mm and a negligible bias. Only a rough knowledge of mean snow grain size $\bar{\phi}$ was required in the inversion procedure. The effects of possible errors on mean snow grain size $\bar{\phi}$ are presented and discussed.**

***Index Terms*—Boreal Ecosystem-Atmosphere Study (BOREAS), Boreal forest, microwave radiometry, snow emission model, snow water equivalent (SWE).**

Manuscript received May 27, 2003; revised April 21, 2004. This work was supported in part by the Environment Canada under the Cryosphere System in Canada Program, in part by the Natural Sciences and Engineering Research Council of Canada, and in part by the Canadian Foundation for Climate and Atmospheric Studies.

V. Roy was with the Centre d'Applications et de Recherches en Télédétection (CARTEL), Université de Sherbrooke, Sherbrooke, QC, J1K 2R1, Canada. He is now with Defence Research and Development Canada, Val-Bélair, QC, G3J 1X5, Canada, (e-mail: vincent.roy@drdc-rddc.gc.ca)

K. Goïta and A. Royer are with the Centre d'Applications et de Recherches en Télédétection (CARTEL), Université de Sherbrooke, Sherbrooke, QC, J1K 2R1, Canada (e-mail: Kalifa.Goita@USherbrooke.ca; Alain.Royer@Usherbrooke.ca).

A. E. Walker and B. E. Goodison are with the Climate Research Branch, Meteorological Service of Canada, Environment Canada, Downsview, ON, M3H 5T4, Canada.

Digital Object Identifier 10.1109/TGRS.2004.832245

I. Introduction

THE MONITORING of snow cover properties (extent, water equivalent, and depth) over large areas is critical for the management of water generated from snow melt. Moreover, in the context of actual climate change studies, the monitoring of these properties at regional scale is of major interest. In fact, the presence of a snow cover modifies significantly the interactions between the surface and the atmosphere [1].

Traditionally, snowpack physical properties are determined from snow coring, at more or less dispersed sampling points. However, this method is ineffective when areas considered are vast, inaccessible, and generally inhabited, as it is the case for the Canadian boreal environment. Moreover, this technique cannot capture the significant snow cover spatial and temporal variability displayed over Canadian landscapes [2] without costly and labor-intensive field campaigns.

During the past 30 years, spaceborne passive microwave observations have been investigated for the estimation of snow extent and water equivalent [3]–[7]. In the passive microwave domain, empirical approaches were developed to estimate snow water equivalent (SWE), most of them based on linear relationships between SWE and the spectral difference of brightness temperatures (generally measured at 37 and 18 or 19 GHz). A review of several approaches is given in [6] and [7]. Progress in algorithm development in Canada [8] led to a near real-time system, processing microwave data and creating snow cover maps for the Canadian Prairies [9], [10]. In forest environments, SWE retrieval is complicated by the attenuation of the ground microwave signal propagating through the canopy and by the vegetation cover contribution to the surface brightness temperature. Goïta *et al.* [5], [11] showed that a single linear relationship cannot be used to estimate SWE in boreal forests and proposed a set of vegetation type-dependent empirical relationships. Also, recent investigations [12], [13] suggested that static empirical relations may be inappropriate in some cases as the slope of the linear relationship relating SWE to the spectral difference of brightness temperatures changes over time (and may even change sign) as an effect of the snow cover seasonal metamorphic evolution.

A number of physically based models have been proposed in the literature to understand the different contributions to the microwave signal [14]–[16]. These types of models provide insight as opposed to empirical models, but they require several

inputs that are not always available in an operational remote sensing context. In this paper, we consider the Helsinki University of Technology (HUT) snow emission model [16] for SWE retrieval because it was developed for boreal forests and has less data requirements for inversion. The study was motivated by the availability of a set of high-quality experimental data, acquired as part of the Boreal Ecosystem-Atmosphere Study (BOREAS) Project in 1994, and by our intent to extend the HUT model applicability to the Canadian environment. So far, this model has been tested in Finland [16]–[18] and northern Russia and Siberia [19].

In Section II, we recall the main basic functions of the HUT model. Then, the study area and the dataset are described in Section III. In Section IV, we investigate the HUT model accuracy in the prediction of microwave surface brightness temperature. As it will be demonstrated in this section, predicted brightness temperatures are biased due to an erroneous modeling of large snow grain effect. In Section V, we propose a modification to the model by using a new semiempirical snow extinction coefficient. Finally, in Section VI, we show that SWE can be retrieved by inversion of the modified HUT snow emission model in the experimental conditions considered in this study.

II. Description of the HUT Snow Emission Model

The approach used in the HUT snow emission model to estimate the brightness temperature of snow-covered ground is based on the following assumptions: 1) the snowpack is a single homogeneous layer and 2) the scattered microwave radiation is mostly concentrated in the forward direction. Thus, the brightness temperature inside a snowpack of depth d, just below the snow–air boundary, can be approximated as follows [16]:

$$T_{\rm b}\left(d^{-},\theta\right) = T_{\rm b}\left(0^{+},\theta\right) e^{-(\kappa_{\rm e}-q\kappa_s)d\cos^{-1}\theta} + \frac{\kappa_{\rm a}T^{\rm snow}}{\kappa_{\rm e}-q\kappa_s}\left(1-e^{-(\kappa_{\rm e}-q\kappa_s)d\cos^{-1}\theta}\right) \quad (1)$$

where θ is the incidence angle, $T_{\rm b}(0^{+},\theta)$ is the brightness temperature at the ground–snow interface, $T^{\rm snow}$ is the snowpack physical temperature, q is an empirical parameter ($q = 0.96$) describing the fraction of intensity scattered in the direction θ, and $\kappa_{\rm e}$, κ_s, and $\kappa_{\rm a}$ are, respectively, the extinction, scattering and absorption coefficients ($\kappa_{\rm e} = \kappa_s + \kappa_{\rm a}$). The effect of snow grain size is described through the extinction coefficient, as determined empirically in [20]

$$\kappa_{\rm e} = 0.0018 f^{2.8}\left(\phi\right)^2 \quad (2)$$

where $\kappa_{\rm e}$ is in decibels, f is the frequency in gigahertz, and ϕ is the snow grain diameter in millimeters. Equation (2) was derived from observations on natural snowpack characterized by grain diameters ranging from 0.2–1.6 mm. The vegetation cover in the model is considered as a single layer that attenuates the snow-covered ground microwave emission and contributes to the microwave signal by its own emission. If we neglect the atmospheric effects, the resulting brightness temperature of a vegetated snow-covered surface as seen from an airborne sensor can be expressed in simple terms as (direction dependence is assumed)

$$T_{\rm b}^{\rm surf} = \left(1-\tau^{\rm veg}\right)T^{\rm veg} + \tau^{\rm veg}T_{\rm b}^{\rm snow} + \left(1-e^{\rm snow}\right)\left(1-\tau^{\rm veg}\right)\tau^{\rm veg}T^{\rm veg} \quad (3)$$

where $T_{\rm b}^{\rm snow}$ corresponds to the brightness of the snowpack ($T_{\rm b}(\mathrm{d}^{-},\theta)$ as shown in (1) times the Fresnel transmission coefficient of the snow–air boundary), $\tau^{\rm veg}$ the vegetation transmittance, $\mathrm{e}^{\rm snow}$ the emissivity of the snowpack, and $T^{\rm veg}$ the physical temperature of the vegetation. The above expression assumes a complete vegetation cover on the ground. In the case of partial vegetation cover, the cover fraction must be considered explicitly in the formulation of the equation.

III. Study Areas and Experimental Dataset

The measurements considered in this study were conducted in the framework of the BOREAS Project [21]. The data were acquired during a winter field campaign (February 5–14, 1994) over both BOREAS northern and southern study sites in Central Canada (Fig. 1, adapted from [22]). The northern study area (NSA) is located west of Thompson, MB (55.54–56.247°N, longitude 97.24–99.05°W), and the southern study area (SSA) is located north of Prince Albert, SK (latitude 53.419–54.319°N, longitude 104.24–106.32°W).

The vegetation cover in NSA is dominated by black spruce with scattered birch and stands of jack pine. The SSA is near the tree line delimiting the boreal forest and the agricultural region that lies to the south. In this site, mixed woods composed of aspen and white spruce are common, with jack pine stands especially on dry sites. In poorly drained areas, bogs support black spruce and tamarack.

During this campaign, passive microwave data were acquired using National Aeronautics and Space Administration Airborne Multichannel Microwave Radiometers (AMMR) onboard a Twin Otter aircraft over several flight lines (see [4]). AMMR operated at frequencies of 18, 37, and 92 GHz, in both horizontal and vertical polarizations, at an altitude of 800 m, viewing at an incidence angle of 45° (spatial resolution of about 80 m). Due to calibration problems for the 92- and 37-GHz channels in horizontal polarization [4], only data at 18 and 37 GHz in vertical polarization were considered in this study. The noise level on these data is approximately ± 5 K. Along the flight lines, detailed ground-based measurements were conducted to characterize surface properties. A total of 112 point measurements were used in this study. These measurements include snow depth, water equivalent, and density over sampling points spaced at 1–2 km intervals, information on vegetation cover type and conditions, as well as snow grain size and temperature profiles. These profiles were integrated (weighted mean using the depth of each layer) in order to derive a mean snow grain size and temperature for each profile.

The observed SWE values ranged from 12–62 mm (average of 42 ± 11 mm). The average snow grain diameter ranged from 1.3–3.2 mm (mean 2.2 ± 0.4 mm). Temperature at the ground-snow interface ranged from -15 °C to -2 °C (mean -9 ± 3 °C), while it ranged from -38 °C to -14 °C (mean -25 ± 5 °C) at

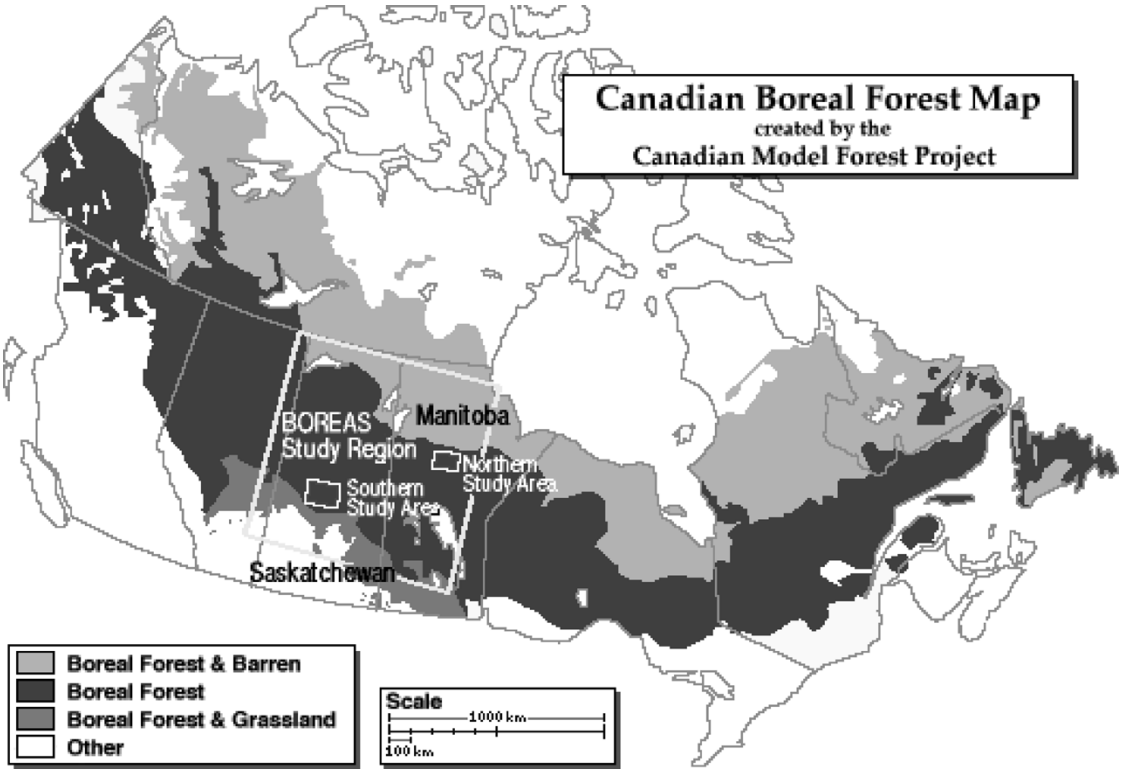

Fig. 1. Map of the BOREAS study area, outlining the southern and northern study areas. Adapted from [22].

the snow–air interface, assuring a dry snow condition. A layer of depth hoar was observed at all sampling points. Its thickness averaged 6 cm overall, but in some cases, the depth hoar layer was as deep as 18 cm. The mean grain diameter in the depth hoar layer ranged from 1.6–6.2 mm, and averaged 3 mm over all sampling points.

The experimental dataset is completed by quantitative information on forest stem volume. This parameter was estimated at each sampling point using forest inventory data [23], [24] by interpolating to the aircraft flight lines. In general, stem volume observed in the SSA (80–230 $m^3 \cdot ha^{-1}$) are higher than those observed in the NSA (80–140 $m^3 \cdot ha^{-1}$).

In the study, the whole dataset was first used in the validation exercise, in which the predicted brightness temperature by the HUT model was compared to the observed value for each sampling point. However, this analysis showed a need for further improvements of the model. Therefore we divided randomly the dataset into two independent subsets. The first one (subset #1) was used for the development of a new extinction function, and the second subset (subset #2) was considered as verification data for validation purposes. Both subsets reflect the experimental conditions depicted in the original dataset, as shown in Table I.

TABLE I
STATISTICAL PROPERTIES OF THE TOTAL EXPERIMENTAL DATASET (112 SAMPLES) AND BOTH SUBSETS (56 SAMPLES)

Property	Dataset	Range	Mean	Std. deviation
Snow density ($g.cm^{-3}$)	Original	[0.08 ; 0.29]	0.16	0.04
	Subset #1	[0.10 ; 0.29]	0.16	0.04
	Subset #2	[0.08 ; [0.28]	0.16	0.04
Snow water equivalent SWE (mm)	Original	[12 ; 62]	41.8	11.1
	Subset #1	[14 ; 60]	41.3	10.2
	Subset #2	[12 ; 62]	42.4	12.0
Integrated grain size ϕ (mm)	Original	[1.28 ; 3.95]	2.15	0.43
	Subset #1	[1.50 ; 3.95]	2.17	0.44
	Subset #2	[1.28 ; 3.13]	2.13	0.43
Vegetation stem volume ($m^3.ha^{-1}$)	Original	[0;231]	106.4	85.7
	Subset #1	[0;231]	96.4	85.7
	Subset #2	[0;231]	116.4	85.3

IV. VALIDATION OF THE HUT SNOW EMISSION MODEL

In order to predict the surface brightness temperature using the HUT model, the ground (humidity, surface roughness, and temperature), snow cover (density, depth, temperature, average grain diameter, and humidity), and vegetation cover (temperature and stem volume) properties must be defined. Using the experimental dataset described earlier, we were able to define most of these parameters, except soil moisture and surface roughness. The vegetation temperature was taken as approximately equal to air temperature [25], [26].

As given by the temperature conditions, the ground was frozen during the experiment. In such case, both the ground humidity and surface roughness have minor influence on its emissivity [27], [28]. A sensitivity analysis performed using the HUT model showed that the exact determination of both soil moisture and surface roughness is not necessary. In fact, emissivity of a dry soil differs by only 1% compared to that of a frozen soil characterized by a moisture volumetric ratio of 30% and surface roughness variation from an RMS height of 1–10 cm leads to an emissivity variation of about 2% at the considered frequencies. Accordingly, both soil moisture and surface roughness were set to constant values, which on the average are assumed representative in the study areas. Soil moisture was set at 30% (volumetric ratio) and surface roughness at an RMS value of 0.02 m.

TABLE II
ERROR ON THE BRIGHTNESS TEMPERATURES MODELED BY THE ORIGINAL HUT SNOW MODEL. MEAN ERROR IS COMPUTED AS $(\Sigma(|T_{\mathrm{b}}^{\mathrm{modeled}} - T_{\mathrm{b}}^{\mathrm{measured}}|)/N)$, AND BIAS IS EQUAL TO $\Sigma(T_{\mathrm{b}}^{\mathrm{modeled}} - T_{\mathrm{b}}^{\mathrm{measured}})/N$. N IS THE NUMBER OF SAMPLES IN THE EXPERIMENTAL DATASET

Channel	Mean error (K)	Bias (K)
8 GHz, pol. V	11.3	10.5
37 GHz, pol. V	28.5	-26.9

Atmospheric effects were neglected, since microwave data were acquired from aircraft flying at low altitude in cold air conditions. The low cold winter sky downwelling brightness temperature (approximately 12 and 25 K at 18 and 37 GHz. respectively, according to the MPM model [29]) coupled with high surface emissivities indicates that the atmospheric contributions can be neglected.

Snow-covered ground brightness temperatures were modeled using the HUT snow emission model and compared to those measured by the airborne radiometers. Errors on the modeled brightness temperature are shown in Table II. The mean error is defined as the mean of the absolute difference between the modeled and measured brightness temperature while the bias is defined as the mean difference between the modeled and measured brightness temperature. As such, a positive bias reflects a systematic overestimation of the brightness temperature by the model. Errors on the modeled brightness temperatures can be caused by the erroneous modeling of the physical processes considered and by uncertainties in input parameters. Also, since the error on the modeled brightness temperatures is defined by comparison to measured brightness temperatures, part of it is linked to the radiometers' accuracy (± 5 K for AMMR).

The values presented in Table II show a bias at both frequencies. A strong underestimation of the brightness temperature at 37 GHz and a slight overestimation at 18 GHz are observed. A similar analysis performed using the horizontally polarized brightness temperature, not shown here, confirmed the absolute calibration problems of the 37-GHz radiometer in horizontal polarization observed by [4].

The fact that the error on the modeled brightness temperatures is larger at 37 GHz than at 18 GHz is an indication that microwave propagation through the snowpack may be erroneously modeled, since the processes at stake are strongly frequency dependent [30].

To locate the error sources, we performed a correlation analysis of the errors relatively to the model input parameters. The results of this analysis are summarized in Table III. It can be clearly seen from this table and also from Fig. 2 that at 18 GHz the errors are significantly (p-value $< 10^{-5}$, at $\alpha = 0.01$ significance level) related to the average snow grain size, with R^2 about 0.46. This remark is also true at 37 GHz ($R^2 = 0.42$). In this latter case, ground and average snow temperature also display significant statistical linkage to the errors, but with a very weak coefficient of determination (R^2 about 0.10).

Since the snow grain size has a much stronger effect than the ground and snow temperature on the emitted brightness temperature, it is difficult to determine if the temperature has a direct effect on the modeled brightness temperature error. This correlation could be indirect in nature, as the snowpack temperature gradient induces metamorphic changes in the snow crystalline structure. This aspect has also been outlined in [31] and [12].

Following the results presented in Table III, we can conclude that the current extinction coefficient function (κ_{e}) in the HUT model, which translates the effect of snow grain size, is largely responsible for the errors in the modeled brightness temperatures at 18 and 37 GHz. This function is not adequate for our experimental conditions. In the next section, a new extinction function is proposed.

V. MODEL IMPROVEMENT

The significant correlations observed between modeled brightness temperatures and observed grain sizes lead us to derive a new extinction coefficient function for the HUT snow emission model. Originally, the extinction coefficient function (2) employed by the HUT model was derived from snow cover transmission loss measurements, using free-space transmission systems in a controlled laboratory environment [20]. The experimental data considered in this study were not acquired in such laboratory-controlled conditions and, thus, may not be used to derive directly a new relation for the extinction coefficient, as in [20]. Therefore, an indirect approach based on the inverse modeling of the HUT snow emission model was used. Values of the extinction coefficient at each individual frequency (18 and 37 GHz) were estimated for all the observations in subset #1. The model input parameters were defined as previously described, except for the snow grain size, a free parameter, whose value was optimized such that the simulated brightness temperature equals the measured brightness temperature. The corresponding extinction coefficients, calculated with (2) using the optimal snow grain diameters, were used together with the measured grain size for each case in the subset to define a new relationship.

This development is based on the scattering properties of snowpack in the microwave frequencies. For the snowpacks considered, the average snow grain size varies between approximately 1 and 3 mm. In that case, the ratio of the wavelength to the particle size ranges approximately from 5–15 at 18 GHz ($\lambda = 16.7$ mm) and from 3–8 at 37 GHz ($\lambda = 8.1$ mm), which led us to consider the Rayleigh scattering theory. Classic radiative transfer theory states that for a spherical particle whose size is small compared to the wavelength, the Rayleigh scattering is proportional to the frequency to the fourth power and to the particle size to the sixth power ($\propto f^4\phi^6$; [32]). This behavior remains valid in the case of a random distribution of particles, as long as the scattered waves superpose themselves in an incoherent manner (independent scattering). When the spacing between particles decreases as density increases, the incoherent superposition condition is no longer respected. This is typical of natural snowpack, composed in first approximation by roughly spherical ice particles densely packed together, where snow grains are allowed to be in contact with each other. Both theoretical [33]–[37] and experimental [20], [38] investigations of the behavior of microwave scattering through a snowpack show that the independent scattering assumption

TABLE III
CORRELATION AND ASSOCIATED p-VALUE (PROBABILITY OF ERROR BASED ON AN F-TEST) BETWEEN THE ERROR ON THE MODELED BRIGHTNESS TEMPERATURES ($T_b^{modeled} - T_b^{measured}$) AT 18 AND 37 GHz AND THE INPUT PARAMETER OF THE ORIGINAL MODEL (USING (2) FOR THE SNOW EXTINCTION COEFFICIENT). * INDICATES STATISTICALLY SIGNIFICANT CORRELATION ($\alpha = 0.01$ SIGNIFICANCE LEVEL)

Input parameter	18 GHz, vertical polarization		37 GHz, vertical polarization	
	R	*p-value*	R	*p-value*
Ground temperature	-0.08	0.4130	-0.33	0.0003 *
Vegetation temperature	-0.14	0.1325	-0.22	0.0184
Average snow temperature	-0.08	0.3889	-0.31	0.0008 *
Snow depth	-0.07	0.4465	-0.06	0.5316
Snow density	0.12	0.2119	-0.02	0.8382
Average snow grain size	-0.68	$< 10^{-5}$ *	-0.65	$< 10^{-5}$ *

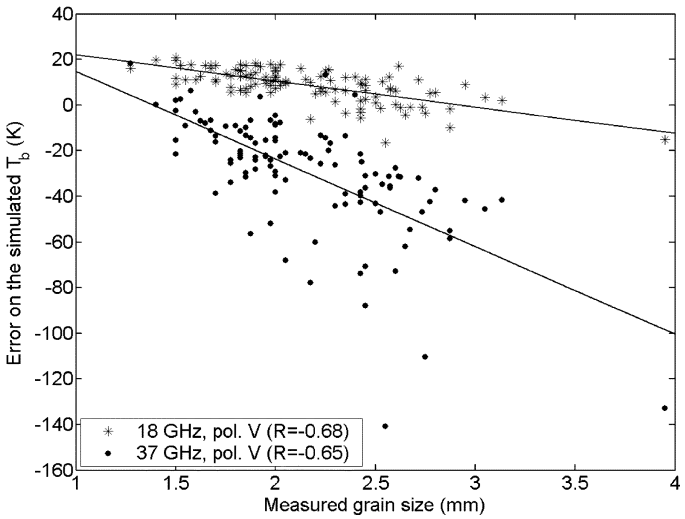

Fig. 2. Relationship between the error on the simulated brightness temperature ($TB^{modeled} - TB^{measured}$) and the measured snow grain size, in vertical polarization at 18 and 37 GHz.

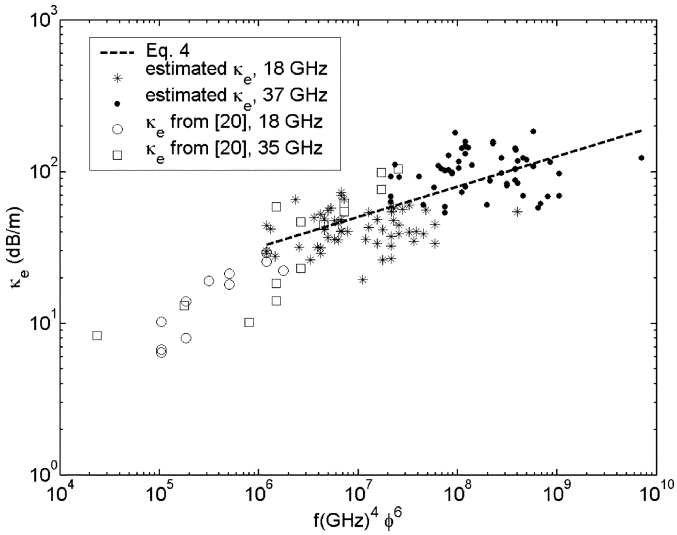

Fig. 3. Snow extinction coefficients estimated from HUT model inversion at 18 and 37 GHz as a function of [f^4 (gigahertz) ϕ^6 (millimeters)]. The dotted line is the derived extinction coefficient function (4). For comparison, the measured extinction coefficient values at 18 and 35 GHz from [20] are also shown. Note that these measurements were not used in the development of (4). Logarithm axes are used.

is not valid. Snow, as a dense medium, exhibits a weaker frequency dependence on scattering than predicted by classical theory. Therefore, we defined a new semiempirical relation for the extinction coefficient as

$$\kappa_e = \gamma \left(f^4 \phi^6\right)^{\delta} \tag{4}$$

where γ and δ are constants determined empirically by least square fitting to the extinction coefficients estimated as described earlier. The empirical constants were found to be $\gamma = 2 \pm 1$ and $\delta = 0.20 \pm 0.04$, effectively translating the departure from classical theory. Fig. 3 shows the newly derived extinction coefficient function (4) as a function of frequency (18 and 37 GHz) and snow grain diameter.

As can be seen visually from Fig. 3, (4) is quantitatively characterized at 18 GHz by a mean error of 14.2 dB/m (relative error of 32% with respect to the average extinction coefficient value) and a bias of 8 dB/m, showing a slight systematic overestimation of the extinction coefficient. At 37 GHz, the mean error is 32.2 dB/m (a relative error of 30%), and a bias of -12.9 dB/m, translating a systematic underestimation of the extinction coefficient. This significant dispersion (large mean error) from the general relation defined in (4) is inherent to the simplifications carried out to model the complex interactions occurring while the radiation is propagating through the snowpack. Since the HUT snow emission model considers the snowpack as homogeneous, it cannot model the impacts of heterogeneities, particularly the vertical distributions of grain size, density, and temperature that generally exist in natural snowpack.

For further comparison, measured extinction coefficient values from [20] are also shown in Fig. 3. It can be seen that the proposed (4) fits well some of the data points, but the dispersion is still important. This fact which can be related to variable snow cover types was also observed when the extinction coefficient function (2) was developed by [20].

Fig. 4 illustrates both relationships (2) and (4) and their ranges of validity in terms of snow grain size, which are, respectively, 0.2–1.6 and 1.3–4 mm. The overlapping zone (1.3–1.6 mm) shows a difference between the two functions (average of 8 dB/m at 18 GHz and 26 dB/m at 37 GHz). This may be explained by differences in experimental conditions (melt–freeze cycles and clustering of snow grain in most snow samples in [20]). In this study, the cluster size is considered instead of individual particle size as in [20]. The effect of clustering of spherical particles on scattering was studied in [33] and showed that

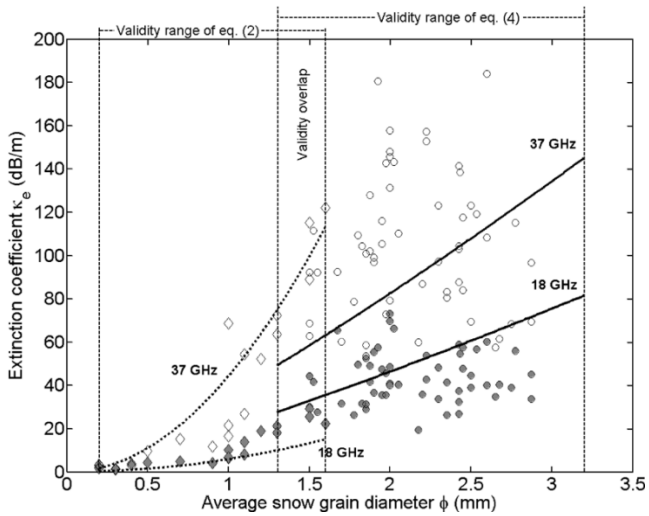

Fig. 4. Illustration of the original and modified extinction functions [respectively (2) and (4)] and their domains of validity in terms of snow grain size. Diamonds correspond to the measured data reported in [20] [extinction coefficient at 35 GHz are extrapolated at 37 GHz using (2)]. Circles correspond to the extinction coefficient estimated from our experimental dataset, using the method described in Section V. Filled and open symbols corresponds to values at 18 and 37 GHz, respectively. Dotted lines represent (2) and black lines are for (4).

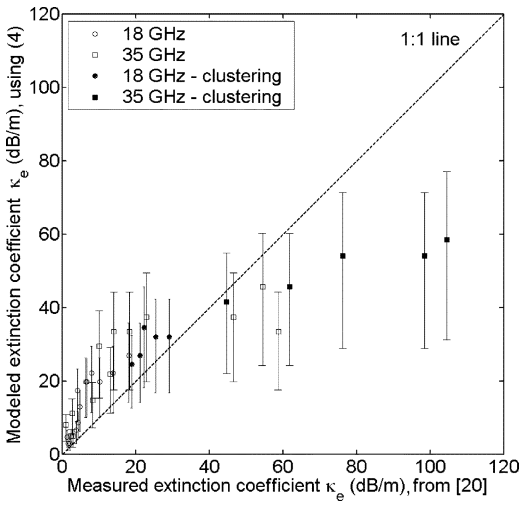

Fig. 5. Comparison between the extinction coefficients modeled using (4) and the measured values reported in [20]. Error bars represent the errors on the modeled values. Black points are samples with clustering.

scattering is stronger for clustered than for nonclustered particles. Accordingly, if clusters are characterized by the size of the individual crystals, as in [20], this will lead to large extinction coefficient for relatively small grain size. On the other hand, if particle size represents the cluster dimension, as it is the case in this study, the same extinction coefficient will be associated to a larger grain size. This may explain the differences observed in Fig. 4 between the measured and modeled extinction coefficients at 37 GHz. In Fig. 5, a direct comparison between estimated κ_e values using (4) and the measured values by [20] effectively shows that (4) underestimates the extinction coefficient for clustered samples. It also overestimates $\kappa_e$for smaller snow grain sizes (≤ 1.1 mm), corresponding to κ_e values under 40 dB/m. Measured κ_e derived from [20] are, thus, not in the

TABLE IV
ERROR ON THE BRIGHTNESS TEMPERATURES MODELED BY THE HUT MODEL USING THE ORIGINAL (2) AND MODIFIED (4) RELATIONS FOR THE EXTINCTION COEFFICIENT. MEAN ERROR IS COMPUTED AS $(\Sigma(|T_b^{\text{modeled}} - T_b^{\text{measured}}|)/N)$, AND BIAS IS EQUAL TO $\Sigma(T_b^{\text{modeled}} - T_b^{\text{measured}})/N$. N IS THE NUMBER OF SAMPLES, TAKEN EXCLUSIVELY FROM SUBSET #2

Channel	Mean error (K)		Bias (K)	
	Original, using (2)	Modified, using (4)	Original, using (2)	Modified, using (4)
18 GHz, pol. V	11.3	5.4	10.5	-1.7
37 GHz, pol. V	28.5	9.3	-26.9	4.7

range of validity in which function (4) was empirically developed (see Fig. 4).

In order to quantify the effect of using (4) instead of (2) to model the snow-covered ground brightness temperature, we repeated the validation process defined earlier (Section IV). Measured brightness temperatures were compared to those modeled with the HUT snow emission model, using both the original (2) and the newly derived (4) extinction coefficient function. Only the verification data from subset #2 (see Table I) were used in the process. Errors on the modeled brightness temperatures are shown in Table IV.

As can be seen from Table IV, using (4) in place of (2) allowed a more accurate modeling of the observed surface brightness temperature, as indicated by the reduced mean error. In fact, the mean error was reduced from approximately 11 to 5 K at 18 GHz and from 29 to 9 K at 37 GHz. In both frequencies the bias was significantly reduced (-1.5 K at 18 GHz and 4.7 K at 37 GHz). These values are in the range of the uncertainty level associated with the microwave measurements (± 5 K). We analyzed the correlations between the errors obtained in this validation process and the input parameters of the model (ground temperature, vegetation temperature, snow temperature, snow depth, density and grain size). We found that when (4) is used the linkage between the simulation errors and the input parameters becomes very weak ($R^2 < 0.21$ in all cases). These results allowed us to conclude that (4) is more adequate than (2) to model the extinction of snow in the experimental context considered in this study. The HUT snow emission model, with the modification proposed to the extinction coefficient function, can simulate the brightness temperature of snow-covered ground in the boreal forest environment considered in central Canada, with a mean error comparable to the radiometer accuracy at 18 and 37 GHz. This indirectly confirms the validity of (4).

Errors on the exact determination of the input parameters and modeling uncertainties could have propagated through and influenced the empirical parameters of the derived equation. As such, the relationship presented in (4) should only be considered valid in the framework of the HUT snow emission model, and not as an independent relationship describing the behavior of the snow extinction coefficient as a function of frequency and grain size. Moreover, (4) is suited to the experimental conditions considered (Table I), i.e., snow grain diameter ranging from 1.3–4 mm, in presence of depth hoar. In particular, (4) is more adapted for modeling the effect of large grain sizes than (2), which predicts larger extinction values in such cases, leading to a systematic underestimation of the brightness temperature at 37 GHz (Table IV). More work is needed in order to derive and

validate a relation covering a larger domain of snow grain sizes in variable snow water equivalent conditions and also including a more complex layering characterization of the snowpack as proposed by [15]. However, simpler models are generally preferred if they are to be inverted to retrieve geophysical parameters from remote sensing observations.

VI. Snow Water Equivalent Retrieval

We investigated the HUT snow emission model's accuracy to retrieve SWE in the study area. Using a model inversion approach, SWE was estimated by minimizing a metric that measures the difference between the airborne observed and HUT modeled brightness temperatures. The metric minimum is found through an iterative process by optimizing two of the model input parameters, namely SWE and snow grain diameter. The set of variables found to minimize the metric is considered as the solution to the inversion problem. All the other input parameters were defined using the experimental measurements from subset #2, as stated in Section III. The same vegetation attenuation function is used as in [16]. Because snow grain size is a difficult parameter to define in an operational context, our goal was to develop an inversion scheme for SWE determination in which knowledge of the grain size is not required. Therefore, in the inversion procedure, we considered the snow grain size as if it was unknown even if it was effectively measured during the campaign. This way, we treated the problem to reflect the more realistic situation where detailed snow measurements as those found in the experimental dataset are not available.

We considered different brightness temperature metrics in order to perform the model inversion to find which one gave the most accurate SWE estimation. The following metrics were considered: 1) Euclidian metrics in the frequency space using only the 18-GHz channel [m_{18}, (5)], only the 37-GHz channel [m_{37}, (6)] and both 18- and 37-GHz channels [$m_{18\&37}$, (7)]; 2) a spectral difference metric [m_{SD}, (8)], as such spectral difference are considered in several empirical SWE retrieval algorithms; and 3) a spectral and polarization metric derived from a metric previously proposed in [16] and [17] for the HUT model inversion [m_{PD}, (9)]. Following the formal approach for the metric derivation presented in [17], the metrics we considered are presented in (5)–(9)

$$m_{18}(\mathrm{SWE},\phi)=\frac{1}{2\sigma^2_{18\ \mathrm{V}}}\left[T^{18\ \mathrm{V}}_{\mathrm{b,observed}}-T^{18\ \mathrm{V}}_{\mathrm{b,modeled}}(\mathrm{SWE},\phi)\right]^2 \tag{5}$$

$$m_{37}(\mathrm{SWE},\phi)=\frac{1}{2\sigma^2_{37\ \mathrm{V}}}\left[T^{37\ \mathrm{V}}_{\mathrm{b,observed}}-T^{37\ \mathrm{V}}_{\mathrm{b,modeled}}(\mathrm{SWE},\phi)\right]^2 \tag{6}$$

$$m_{18\&37}(\mathrm{SWE},\phi)=m_{18}(\mathrm{SWE},\phi)+m_{37}(\mathrm{SWE},\phi) \tag{7}$$

$$m_{\mathrm{SD}}(\mathrm{SWE},\phi)=\frac{1}{2\sigma^2_{18\ \mathrm{V}-37\ \mathrm{V}}}\left\{\left[T^{18\ \mathrm{V}}_{\mathrm{b,observed}}-T^{37\ \mathrm{V}}_{\mathrm{b,observed}}\right]-\left[T^{18\ \mathrm{V}}_{\mathrm{b,modeled}}(\mathrm{SWE},\phi)-T^{37\ \mathrm{V}}_{\mathrm{b,modeled}}\cdot(\mathrm{SWE},\phi)\right]\right\}^2 \tag{8}$$

$$m_{\mathrm{SPD}}(\mathrm{SWE},\phi)=\frac{1}{2\sigma^2_{18\ \mathrm{V}-18\ \mathrm{H}}}\left\{\left[T^{18\ \mathrm{V}}_{\mathrm{b,observed}}-T^{18\ \mathrm{H}}_{\mathrm{b,observed}}\right]-\left[T^{18\ \mathrm{V}}_{\mathrm{b,modeled}}(\mathrm{SWE},\phi)-T^{18\ \mathrm{H}}_{\mathrm{b,modeled}}\cdot(\mathrm{SWE},\phi)\right]\right\}^2+m_{\mathrm{SD}}(\mathrm{SWE},\phi). \tag{9}$$

TABLE V
Mean Error and Bias on the Retrieved SWE by Inversion of the HUT Model Using (4) for the Snow Extinction Coefficient. For Comparison Purposes, the Results Using the Original Extinction Coefficient Function (2) Are Presented in Parentheses. Optimal Accuracy (Smallest Mean Error and Bias in Absolute Value) is Highlighted in Bold, and Correspond to the $m_{18\&37}$ Metric (7) Using the Average Snow Grain Size Information (10)

Metric	Mean error (mm)		Bias (mm)	
	Tb only metric	Tb + ϕ metric (10)	Tb only metric	Tb + ϕ metric (10)
m_{18}	15.7 (45.5)	10.1 (34.3)	13.9 (45.0)	-1.7 (33.8)
m_{37}	29.4 (16.7)	13.8 (21.3)	29.4 (11.6)	7.7 (-20.8)
$m_{18\&37}$	no convergence	**10.0** (16.2)	no convergence	**1.0** (-13.7)
m_{SD}	33.9 (19.6)	22.8 (34.6)	3.4 (-7.1)	15.2 (-34.6)
m_{SPD}	24.0 (19.0)	17.3 (34.4)	-22.6 (-16.0)	3.5 (-34.4)

T^{fp}_{b} is the brightness temperature at frequency f in polarization p, and σ_d is the distribution variance of observed brightness temperature or function of observed brightness temperature in case of (8) and (9).

Estimation of the SWE using the described iterative inversion process was performed using metrics (5)–(9). The retrieved SWE values were compared to those that were directly measured at ground level. Mean error and bias on the retrieved SWE are presented in Table V, under the columns "T_{b} only metric." SWE retrieval accuracy using the modified model [i.e., using (4)] is compared to the accuracy of the original model, for the experimental conditions considered. The SWE retrieval accuracy obtained using metrics (5)–(9) was not particularly promising as large errors (in the order of 20–30 mm) and strong biases were observed.

This poor accuracy is linked to the predominant effect of grain size on the emitted brightness temperature. In order to overcome this problem, we introduced in the metric a direct dependency on a mean observed snow grain size that describes, in general, the physical condition of the snowpack considered. This approach was used in previous works [16], [17] involving SWE retrieval by HUT model inversion. In this approach, SWE is estimated by minimizing a metric that measures the difference between both the airborne observed and HUT modeled brightness temperatures and the observed and modeled snow grain size (10)

$$m'_{\alpha}(\mathrm{SWE},\phi)=m_{\alpha}+\frac{1}{2\sigma^2_{\phi}}\left(\phi-\bar{\phi}\right)^2 \tag{10}$$

where $m\alpha$ are the metrics presented in (5)–(9), which depend only on brightness temperatures, σ_ϕ is the distribution variance of the observed snow grain diameter, ϕ is the modeled snow grain size, and $\bar{\phi}$ is a mean snow grain diameter, supposed constant over a finite time and space domain (a single value was used in the present study; see Table I). Mean errors and biases on retrieved SWE using metrics (5)–(9) with explicit dependency on snow grain size are presented in Table V, under the columns "$T_{\mathrm{b}}+\phi$ metric." When compared to the original model (in parentheses in Table V), results presented in Table V show that replacing the original extinction coefficient function (2) with the newly derived expression (4) generally enhances the accuracy of SWE retrieval.

From Table V, we can see that a metric including direct dependency on snow grain size generally allows a more accurate SWE retrieval. The metric found to provide the best SWE estimation

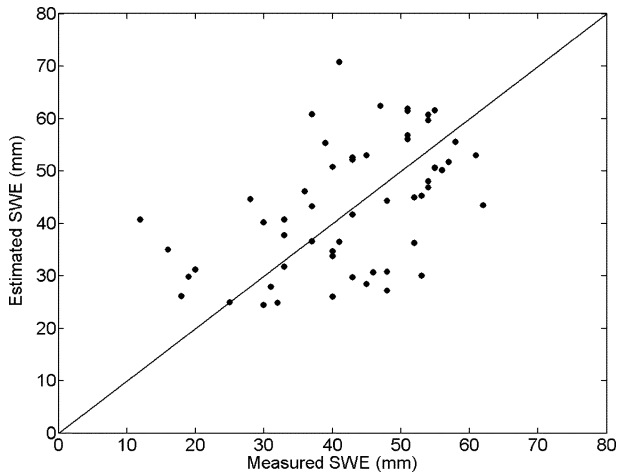

Fig. 6. Comparison between measured and estimated SWE, using the HUT snow emission model with the newly derived extinction coefficient function (4), and the Euclidian metric given in (7) with a constant *a priori* known mean snow grain size.

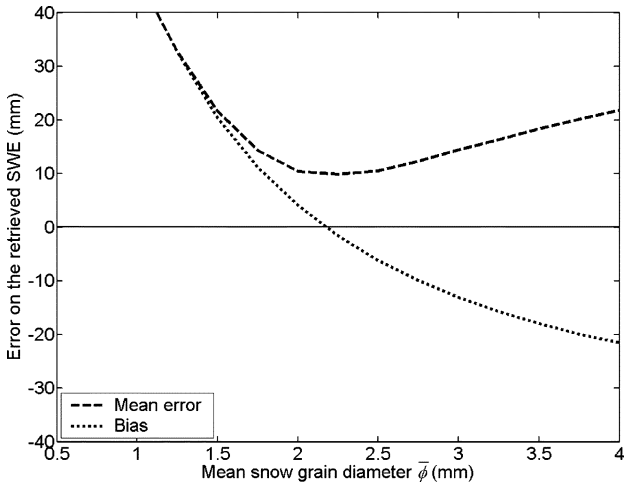

Fig. 7. Sensitivity of the mean error and the bias of retrieved SWE to the mean snow grain diameter $\bar{\phi}$.

(smallest mean error and bias in absolute value in Table V) is the Euclidian metric presented in (7) with inclusion of mean snow grain size information through (10). Results for this metric are highlighted in bold characters in Table V. This is an indication that brightness temperatures, modeled using the modified HUT snow emission model, are precise enough for a direct inversion scheme instead of using spectral and/or polarization difference metrics. Using this metric, our results show that, in the given experimental conditions, SWE may be retrieved with a precision of about 25% (mean error $= 10$ mm for a mean observed SWE $= 42.4$ mm), in an unbiased way (no systematic under- or overestimation of SWE). Fig. 6 presents a graphical comparison between the estimated and the measured SWE using the approach described previously.

A drawback to this approach taken to retrieve SWE is that it explicitly requires a priori information on the mean snow grain size $\bar{\phi}$ in (10). We analyzed the dependence of the retrieved SWE accuracy on the exact determination of $\bar{\phi}$. The behaviors of the mean error and the corresponding bias as a function of $\bar{\phi}$ are illustrated in Fig. 7.

It can be observed from Fig. 7 that at approximately $\bar{\phi} = 2.2$ mm the mean error is minimum and bias is null. This optimal value for $\bar{\phi}$ reflects experimental conditions (Table I). An overestimation of $\bar{\phi}$ will lead to a negative bias, which represents a systematic underestimation of the SWE, and inversely an underestimation of $\bar{\phi}$ will lead to a positive bias. Quantitatively and for the experimental conditions considered, a variation on the chosen mean snow grain diameter of $+0.5$ mm ($\sim 20\%$) from the optimal value will increase the mean error on SWE by 1.8 mm ($\sim 18\%$) and introduce a bias of -8.9 mm. On the other hand, a variation of $\bar{\phi}$ of -0.5 mm will increase the mean error on SWE by 6.3 mm with a 13.7-mm bias. According to these results, we can conclude that SWE may be retrieved accurately using the defined methodology as long as $\bar{\phi}$ describes roughly the physical condition of the considered snowpack.

In the present investigation, the mean grain size $\bar{\phi}$ determination was possible using the data collected during the field campaign. However, in the context of operational snow cover monitoring, the direct measurement of $\bar{\phi}$ is not feasible. Physically based snow metamorphism models like SNTHERM [14], [39] and CROCUS [40] or empirical model [31] may be used to predict a mean snow grain size from meteorological data and/or numerical weather forecasts. On the other hand, the mean grain size may be estimated by assimilating spaceborne microwave measurements with ground-based snow depth measurements conducted at meteorological stations dispersed over the study area, as investigated in [41]. In future work, these two approaches should be investigated into more detail in order to extend the methodology presented in this paper to operational SWE retrieval from spaceborne microwave measurements. Also, the influence of the vegetation cover attenuation function, which is empirically defined in the HUT snow emission model, should be further analyzed.

VII. Conclusion

In this paper, we presented a validation of the HUT snow emission model in a Canadian boreal forest environment, using data from the winter 1994 BOREAS field campaign. The original model validation uncovered a systematic modeling error, characterized by a significant correlation between errors on simulated brightness temperatures and snow grain size, which controls the snow cover extinction behavior in the HUT model. Therefore, we proposed a different semiempirical relationship, based on an empirical correction to the Rayleigh scattering expression. Using the newly derived relation for the extinction coefficient leads to more precise estimations of brightness temperatures at 18 and 37 GHz in vertical polarization, comparable to the radiometers accuracies.

Having validated the model for the experimental conditions prevailing during the field campaign, we investigated the accuracy of the modified HUT model to estimate SWE using an iterative inversion approach. We demonstrated that SWE estimation is possible using the modified HUT model, with a mean error of 10 mm and a negligible bias. We also illustrated the sensitivity of the inversion methodology to a precise determination of the mean snow grain diameter $\bar{\phi}$. The accuracy on SWE retrieval by inversion remains good even with an uncertainty of ± 0.5 mm on the mean grain size. This allows us to conclude that

the HUT snow emission model with an appropriate snow extinction coefficient expression is usable for the estimation of SWE in the Canadian boreal environment. However, more work is still needed to validate the SWE retrieval methodology for different experimental conditions, in order to complement the techniques actually used to retrieve SWE over the vast and highly variable landscapes of Canada.

ACKNOWLEDGMENT

The authors gratefully acknowledge J. Pulliainen (Helsinki University of Technology, Finland) for providing the HUT snow emission model source codes. Support from BOREAS Science Staff is also fully appreciated.

REFERENCES

[1] T. P. Barnett, L. Dumenil, W. Schlese, E. Roeckner, and M. Latif, "The effect of Eurasian snow cover on regional and global climate variations," *J. Atmos. Sci.*, vol. 46, pp. 61–685, 1989.

[2] R. D. Brown and R. O. Braaten, "Spatial and temporal variability of Canadian monthly snow depths, 1946–1995," *Atmos. Ocean*, vol. 36, pp. 37–45, 1998.

[3] B. E. Goodison and A. E. Walker, "Canadian development and use of snow cover information from passive microwave satellite data," in *Passive Microwave Remote Sensing of Land-Atmosphere Interactions*, B. J. Choudhury, Ed. Utrecht, The Netherlands: VSP, 1994, pp. 245–262.

[4] A. T. C. Chang, J. L. Foster, D. K. Hall, B. E. Goodison, A. E. Walker, J. R. Metcalfe, and A. Harby, "Snow parameters derived from microwave measurements during the BOREAS winter field campaign," *J. Geophys. Res.*, vol. 102, no. D24, pp. 29 663–29 671, 1997.

[5] K. Goïta, A. E. Walker, and B. E. Goodison, "Algorithm development for the estimation of snow water equivalent in the boreal forest using passive microwave data," *Int. J. Remote Sens.*, vol. 24, pp. 1097–1102, 2003.

[6] R. Singh and T. Y. Gan, "Retrieval of snow water equivalent using passive microwave brightness temperature data," *Remote Sens. Environ.*, vol. 74, pp. 275–286, 2000.

[7] M. T. Hallikainen and P. A. Jolma, "Comparison of algorithms for retrieval of snow water equivalent from Nimbus-7 SSMR data in Finland," *IEEE Trans. Geosci. Remote Sensing*, vol. 30, pp. 124–131, Jan. 1992.

[8] A. E. Walker and B. E. Goodison, "Challenges in determining snow water equivalent over Canada using microwave radiometry," in *Proc. IGARSS*, Honolulu, HI, 2000, pp. 1551–1554.

[9] B. E. Goodison, "Determination of areal snow water equivalent on the Canadian prairies using passive microwave satellite data," in *Proc. IGARSS*, vol. 3, Vancouver, BC, Canada, 1989, pp. 1243–1246.

[10] F. Thirkettle, A. E. Walker, B. E. Goodison, and D. Graham, "Canadian prairie snow cover maps from real-time passive microwave data: From satellite data to user information," in *Proc. 14th Can. Symp. Remote Sensing*, Calgary, AB, Canada, May 6–10, 1991, pp. 172–176.

[11] K. Goïta, A. E. Walker, B. E. Goodison, and A. T. C. Chang, "Estimation of snow water equivalent in the boreal forest using passive microwave data," in *Proc. Int. Symp. Geomatics Era of Radarsat*, Ottawa, ON, Canada, May 24–30, 1997.

[12] S. Rosenfeld and N. Grody, "Anomalous microwave spectra of snow cover observed from Special Sensor Microwave/Imager measurements," *J. Geophys. Res.*, vol. 105, no. D11, pp. 14 913–14 925, 2000.

[13] ——, "Metamorphic signature of snow revealed in SSM/I measurements," *IEEE Trans. Geosci. Remote Sensing*, vol. 38, pp. 53–63, Jan. 2000.

[14] C.-T. Chen, B. Nijssen, J. Guo, L. Tsang, A. W. Wood, J.-N. Hwang, and D. P. Lettenmair, "Passive microwave remote sensing of snow constrained by hydrological simulations," *IEEE Trans. Geosci. Remote Sensing*, vol. 39, pp. 1744–1756, Aug. 2001.

[15] A. Wiesmann and C. Mätzler, "Microwave emission model of layered snowpacks," *Remote Sens. Environ.*, vol. 70, pp. 307–316, 1999.

[16] J. T. Pulliainen, J. Grandell, and M. T. Hallikainen, "HUT snow emission model and its applicability to snow water equivalent retrieval," *IEEE Trans. Geosci. Remote Sensing*, vol. 37, pp. 1378–1390, May 1999.

[17] J. T. Pulliainen and M. T. Hallikainen, "Retrieval of regional snow water equivalent from space-borne passive microwave observations," *Remote Sens. Environ.*, vol. 75, pp. 76–85, 2001.

[18] N. Kruopis, J. Praks, A. N. Arslan, H. M. Alasalmi, J. T. Koskinen, and M. T. Hallikainen, "Passive microwave measurements of snow-covered forest areas in EMAC'95," *IEEE Trans. Geosci. Remote Sensing*, vol. 37, pp. 2699–2705, Nov. 1999.

[19] M. Tedesco, P. Pampaloni, J. Pulliainen, and M. T. Hallikainen, "Classification and retrieval of dry snow parameters by means of SSM/I data and artifical neural networks," in *Proc. IGARSS*, Toulouse, France, 2003.

[20] M. T. Hallikainen, F. T. Ulaby, and T. Deventer, "Extinction behavior of dry snow in the 18 to 90 GHz range," *IEEE Trans. Geosci. Remote Sensing*, vol. GE-25, pp. 737–745, 1987.

[21] P. P. Sellers, F. Hall, H. Margolis, B. Kelly, D. Baldocchi, G. den Hartog, J. Cihlar, M. G. Ryan, B. E. Goodison, P. P. Crill, K. J. Ranson, D. Lettenmaier, and D. E. Wickland, "The Boreal Ecosystem-Atmosphere Study (BOREAS): An overview and early results from the 1994 field year," *Bull. Amer. Meteorol. Soc.*, vol. 76, pp. 1549–1577, 1995.

[22] J. Newcomer, D. Landis, S. Conrad, S. Curd, K. Huemmrich, D. Knapp, A. Morrell, J. Nickeson, A. Papagno, D. Rinker, R. Strub, T. Twine, F. Hall, and P. Sellers. (2000) Collected data of the Boreal Ecosystem-Atmosphere Study. Oak Ridge Nat. Lab., Distribut. Active Archive Center, Oak Ridge, TN. [Online]. Available: http://www-eosdis.ornl.gov.

[23] D. H. Halliwell and M. J. Apps, "Boreal Ecosystem-Atmosphere Study (BOREAS) biometry and auxillary sites: Overstory and understory data," Northern Forestry Centre, Edmonton, AB, Canada, 1997.

[24] ——, "Boreal Ecosystem-Atmosphere Study (BOREAS) biometry and auxillary sites: Locations and descriptions," Northern Forestry Centre, Edmonton, AB, Canada, Rep. Can. For. Service, 1997.

[25] M. Fily, A. Royer, K. Goïta, and C. Prigent, "A simple method for land surface temperature and fraction of water surface determination from satellite microwave brightness temperatures in sub-arctic areas," *Remote Sens. Environ.*, vol. 85, pp. 328–338, 2003.

[26] J. Smyth and K. Goïta, "Statistical analysis of the impact of temperature and vegetation cover on snow water equivalent estimation using SSM/I data over New Brunswick and Southern Quebec," in *Proc. 56th Eastern Snow Conf.*, Fredericton, NB, Canada, 1999, pp. 91–97.

[27] M. Dobson, F. T. Ulaby, M. T. Hallikainen, and M. El-Rayes, "Microwave dielectric behavior of wet soil—Part II: Dielectric mixing models," *IEEE Trans. Geosci. Remote Sensing*, vol. GE-23, pp. 35–46, Jan. 1985.

[28] U. Wegmüller and C. Mätzler, "Rough bare soil reflectivity model," *IEEE Trans. Geosci. Remote Sensing*, vol. 37, pp. 1391–1395, May 1999.

[29] H. J. Liebe, "MPM—An atmospheric millimeter-wave propagation model," *Int. J. Infr. Millim. Waves*, vol. 10, pp. 632–650, 1989.

[30] F. T. Ulaby, R. K. Moore, and A. K. Fung, *Microwave Remote Sensing, Active and Passive*. Norwood, MA: Artech House, 1986, vol. III, From Theory to Applications, p. 2162.

[31] E. G. Josberger and N. M. Mognard, "A passive microwave snow depth algorithm with a proxy for snow metamorphism," *Hydrol. Process.*, vol. 16, pp. 1557–1568, 2002.

[32] J. D. Jackson, *Classical Electrodynamics*. New York: Wiley, 1975, pp. 456–462.

[33] L. M. Zurk, L. Tsang, K. H. Ding, and D. P.-P. Winebrenner, "Monte Carlo simulations of the extinction rate of densely packed spheres with clustered and non clustered geometries," *J. Opt. Soc. Amer. A*, vol. 12, pp. 1772–1781, 1995.

[34] L. M. Zurk, L. Tsang, and D. P.-P. Winebrenner, "Scattering properties of dense media from Monte Carlo simulations with application to active remote sensing of snow," *Radio Sci.*, vol. 31, pp. 803–819, 1996.

[35] L. Tsang, C.-T. Chen, A. T. C. Chang, J. Guo, and K.-H. Ding, "Dense media radiative transfer theory based on quasi crystalline approximation with applications to passive microwave remote sensing of snow," *Radio Sci.*, vol. 35, pp. 731–749, 2000.

[36] J. Guo, L. Tsang, K.-H. Ding, A. T. C. Chang, and C.-T. Chen, "Frequency dependence of scattering by dense media of small particles based on Monte Carlo simulations of Maxwell equations," *IEEE Trans. Geosci. Remote Sensing*, vol. 40, pp. 153–161, Jan. 2002.

[37] C.-T. Chen, L. Tsang, J. Guo, A. T. C. Chang, and K. H. Ding, "Frequency dependence of scattering and extinction of dense media based on three-dimensional simulations of Maxwell's equations with application to snow," *IEEE Trans. Geosci. Remote Sensing*, vol. 41, pp. 1844–1852, Aug. 2003.

[38] A. Wiesmann, C. Mätzler, and T. Weise, "Radiometric and structural measurements of snow samples," *Radio Sci.*, vol. 33, pp. 273–289, 1998.

[39] L. L. Wilson, L. Tsang, J.-N. Hwang, and C.-T. Chen, "Mapping snow water equivalent by combining a spatially distributed snow hydrology model with passive microwave remote-sensing data," *IEEE Trans. Geosci. Remote Sensing*, vol. 37, pp. 690–704, Mar. 1999.

[40] E. Brun, P. David, M. Sudul, and G. Brugnot, "A numerical model to simulate snow-cover stratigraphy for operational avalanche forecasting," *J. Glaciol.*, vol. 38, pp. 13–22.

[41] J. Pulliainen, M. Takala, and M. T. Hallikainen, "Assimilation of spaceborne microwave radiometer and discrete ground-based data in snow depth mapping: A case study for Northern Eurasia," in *Proc. IGARSS*, Toronto, ON, Canada, 2002.

Vincent Roy (S'02–M'04) received the B.Sc. degree in physics and the M.Sc. degree in remote sensing from the Université de Sherbrooke, Sherbrooke, QC, Canada, in 1999 and 2003, respectively.

Between 2000 and 2003, he was a Research Assistant in the Department of Geography and Remote Sensing, University of Sherbrooke, where his main interest was remote sensing of snow in forested areas. In 2003, he participated in winter field expeditions in Saskatchewan and Quebec, Canada. Since April 2003, he has been a Defence Scientist in remote sensing at Valcartier Defence Research and Development Canada (DRDC) Laboratory, Val-Bélair, QC. His work currently focuses on the exploitation of hyperspectral data.

Mr. Roy received the Canadian Governor General's Academic Medal in 2003.

Kalifa Goïta received the Eng. Degree in surveying engineering from the École Nationale d'Ingénieurs, Bamako, Mali, in 1987, and the M.Sc. and Ph.D. degrees in remote sensing from the Université de Sherbrooke, Sherbrooke, QC, Canada, in 1991 and 1995, respectively.

He was a Postdoctoral Fellow at the Climate Research Branch of Environment Canada, Toronto, ON, from 1995 to 1997. From 1997 to 2002, he was with the Faculty of Forestry, Université de Moncton, Moncton, NB, Canada, as Professor of remote sensing and GIS. Since June 2002, he has been a Professor of geomatics with the Université de Sherbrooke and a Researcher at the Centre d'Applications et de Recherche en Télédétection (CARTEL). His research interests include passive microwave remote sensing of snow, remote sensing of ecological indicators for forestry applications, and the development of dynamic geographic information systems for environmental monitoring. He is a member of the Cryosphere System in Canada (CRYSYS) research group.

Dr. Goïta received the Canadian Remote Sensing Society award for the best Ph.D. thesis in remote sensing in 1995. He is a member of the association Québécoise de Télédétection.

Alain Royer received the Doctorate degree in geophysics from the University J. Fourier, Grenoble, France, in 1981.

From 1983 to 1988, he was a Natural Sciences and Engineering Research Council Fellow at the Centre d'Applications et de Recherches en Télédétection (CARTEL) of the Université de Sherbrooke, Sherbrooke, QC, Canada. In 1988, he became a member of the professorial team of the Université de Sherbrooke. From 2000 to 2003, he was the Head of CARTEL. His research interests are environmental geophysics from space, including the development of surface parameter retrieval algorithms from remote sensing data applied to climate change analysis. He is involved in the Canadian Cryosphere System project, in the framework of the Canadian CliC program.

Anne E. Walker received the B.A. and M.A. degrees in geography from Carleton University, Ottawa, ON, Canada, in 1984 and 1986, respectively.

She has been a Physical Scientist with the Climate Research Branch, Meteorological Service of Canada, Downsview, ON, since 1990. She leads a scientific research program that is focused on developing the use of passive microwave data to derive, analyze, and model geophysical variables (e.g., snow cover, lake ice, soil moisture) in support of analyses of climate variability and change. She is currently a NASA EOS Co-Investigator with the interdisciplinary investigation entitled Cryosphere System in Canada (CRYSYS), responsible for snow cover and lake ice research activities. Since 1999, she has been a member of the Polar User Working Group (UWG) for the EOS Snow and Ice Distributed Active Archive Center at National Snow and Ice Data Center, Boulder, CO, providing advice on Distributed Active Archive Center activities such as archiving/production of cryospheric datasets from EOS sensors and data management issues.

Barry E. Goodison, photograpy and biography not available at the time of publication.